Shell corrections for finite depth potentials: Particle continuum effects

T. Vertse,[1–3], A.T. Kruppa,[1], R.J. Liotta,[3] W. Nazarewicz,[4–6] N. Sandulescu,[3,7], and T.R. Werner[6]

[1]*Institute of Nuclear Research of the Hungarian Academy of Sciences*
P. O. Box 51, H-4001, Debrecen, Hungary

[2]*Joint Institute for Heavy Ion Research*
Oak Ridge National Laboratory, P.O. Box 2008, Oak Ridge, Tennessee 37831

[3]*Royal Institute of Technology, Physics Department Frescati*
Frescativagen 24, S-10405, Stockholm, Sweden

[4]*Department of Physics and Astronomy, University of Tennessee*
Knoxville Tennessee 37996

[5]*Physics Division, Oak Ridge National Laboratory*
P.O. Box 2008, Oak Ridge, Tennessee 37831,

[6]*Institute of Theoretical Physics, Warsaw University, ul. Hoża 69, PL-00681, Warsaw, Poland*

[7]*Institute of Atomic Physics, Box MG-6, Bucharest, Romania*

Abstract

Shell corrections of finite, spherical, one-body potentials are analyzed using a smoothing procedure which properly accounts for the contribution from the particle continuum, i.e., unbound states. Since the plateau condition for the smoothed single-particle energy seldom holds, a new recipe is suggested for the definition of the shell correction. The generalized Strutinsky smoothing procedure is compared with the results of the semi-classical Wigner-Kirkwood expansion. A good agreement has been found for weakly bound nuclei in the vicinity of the proton drip line. However, some deviations remain for extremely neutron-rich systems due to the pathological behavior of the semi-classical level density around the particle threshold.

PACS number(s): 21.10.Dr, 21.10.Ma, 21.60.-n

I. INTRODUCTION

Positive-energy eigenstates of the average single-particle potential are very important for the description of nuclei close to the particle drip lines where the Fermi level approaches zero (see Ref. [1] and references quoted therein), and in analysis of highly excited nuclear modes such as giant resonances [2,3]. With the advent of radioactive nuclear beams, of particular interest are masses of weakly bound nuclei with extreme N/Z ratios. For these nuclei, important for both nuclear structure and astrophysics, special care should be taken when dealing with the particle continuum, which strongly influences many nuclear properties, including global ones (e.g., masses, radii, shapes) as well as nuclear dynamics (i.e., excitation modes).

In a previous paper [4], a macroscopic-microscopic method was applied to nuclei far from the beta stability line. It has been demonstrated that the systematic error in binding energies, due to the particle continuum, can be as large as several MeV at the neutron drip line; hence it can seriously affect theoretical mass predictions for nuclei far from stability. This error depends weakly on deformation, thus suggesting a possibility of re-normalizing potential energy surfaces at the spherical shape.

In this paper, the effect of the particle continuum on the shell correction (the quantal contribution to the total energy in the macroscopic-microscopic approach) is investigated by solving the Schrödinger equation in the complex energy plane. The new procedure allows for the direct treatment of both narrow resonances and the smooth continuum background when calculating the single-particle level density.

The paper is organized as follows. Section II contains a brief review of the shell-correction method in terms of the single-particle level density. The semi-classical approach is discussed in Sec. III. Section IV describes the modified Strutinsky re-normalization procedure which takes care of the continuum effects. The results of the calculations are contained in Sec. V. Finally, conclusions are given in Sec. VI. The threshold behavior of the semi-classical level density is discussed in Appendix A.

II. SHELL CORRECTION AND SINGLE-PARTICLE LEVEL DENSITY

In the standard macroscopic-microscopic approach [5–8], the shell correction

$$\delta E = E_{\rm s.p.} - \tilde{E}_{\rm s.p.} \tag{1}$$

is the difference between the total single-particle energy $E_{\rm s.p.}$,

$$E_{\rm s.p.} = \sum_{i-{\rm occ}} \varepsilon_i \ , \tag{2}$$

and the smooth single-particle energy $\tilde{E}_{\rm s.p.}$. The shell correction represents the fluctuating part of the binding energy resulting from the single-particle shell structure.

For the sake of simplicity, we shall restrict our discussion to spherically symmetric nuclei and assume that the single-nucleon energy spectrum is that of a one-body Hamiltonian $\hat{H} = T + V$ with a finite, local, and spherically symmetric potential $V(r)$. Since the spectrum

of H contains both bound ($\varepsilon_i < 0$) and unbound ($\varepsilon > 0$) eigenvalues, the single-particle level density is the sum of the discrete and continuum contributions [9–13]

$$g(\varepsilon) = \sum_i (2j_i + 1)\delta(\varepsilon - \varepsilon_i) + g_{\rm c}(\varepsilon). \tag{3}$$

The continuum part, $g_{\rm c}(\varepsilon)$, is defined in terms of the scattering phase shifts $\delta_{lj}(\varepsilon)$

$$g_{\rm c}(\varepsilon) = \frac{1}{\pi} \sum_{l,j} (2j + 1) \frac{d\delta_{lj}(\varepsilon)}{d\varepsilon}. \tag{4}$$

In the shell-correction method [5,6] the smooth energy $\tilde{E}_{\rm s.p.}$ is calculated by employing the smooth level density $\tilde{g}(\varepsilon)$ obtained from $g(\varepsilon)$ by folding with a smoothing function $f(x)$:

$$\tilde{g}(\varepsilon) = \frac{1}{\gamma} \int_{-\infty}^{+\infty} d\varepsilon' \; g(\varepsilon') f\left(\frac{\varepsilon' - \varepsilon}{\gamma}\right). \tag{5}$$

The folding function $f(x)$ can be written as a product of a weighting function and a curvature correction polynomial of the order p=$2M$ [6]. The smoothing procedure should be unambiguous, i.e., the averaging should leave the smooth part of the level density untouched (the so-called self-consistency condition for the Strutinsky smoothing). This defines a curvature correction polynomial for any specific choice of weighting function. In this study, a Gaussian weighting function, $\frac{1}{\sqrt{\pi}} \exp(-x^2)$ has been used. The corresponding curvature function is an associated Laguerre polynomial $L_M^{1/2}(x^2)$. This choice guarantees the self-consistency condition for $\tilde{g}(\varepsilon)$ if the smooth level density behaves as a polynomial of degree $2M + 1$ or lower in ε.

The smoothed level density (5) defines both the smooth single-particle energy

$$\tilde{E}_{\rm s.p.} = \int_{-\infty}^{\tilde{\lambda}} \varepsilon \, \tilde{g}(\varepsilon) d\varepsilon, \tag{6}$$

and the smoothed Fermi level $\tilde{\lambda}$. The latter is obtained from the particle number equation:

$$N = \int_{-\infty}^{\tilde{\lambda}} \tilde{g}(\varepsilon) d\varepsilon, \tag{7}$$

where N is the total number of particles (i.e. protons or neutrons). The smoothing range γ should be greater than the average energy distance between neighboring major shells, $\hbar\Omega \approx 41/A^{1/3}$ MeV [14].

Since the result of the smoothing procedure should not depend on the actual form of the smoothing function, in particular on the smoothing range γ and the order p of curvature correction, the smooth energy should satisfy the so-called *plateau condition*:

$$\frac{\partial \tilde{E}_{\rm s.p.}}{\partial \gamma} = 0 \quad , \frac{\partial \tilde{E}_{\rm s.p.}}{\partial p} = 0. \tag{8}$$

For infinite potentials such as a harmonic oscillator or a deformed Nilsson potential, one can always find an interval of the smoothing parameters γ and p in which the smooth energy,

hence the shell correction, is practically independent of the values γ and p [12,15]. For finite-depth potentials, additional complications arise due to the presence of the continuum contribution, Eq. (4) (see discussion in Refs. [4,2] and references quoted therein). In most calculations applying the shell-correction approach, the continuum is treated approximately by using the *quasi-bound states*, i.e., the states resulting from the diagonalization of a finite potential in a large harmonic oscillator basis [7]. However, for light and weakly bound nuclei, the plateau condition (8) usually does not hold [4].

III. SEMI-CLASSICAL TREATMENT OF SHELL CORRECTION

A possible alternative to Strutinsky's smoothing procedure is the semi-classical averaging based on the Wigner-Kirkwood expansion [15–21]. In Ref. [17] the equivalence between the Strutinsky approach and the Wigner-Kirkwood (WK) expansion has been demonstrated. It is important to note that this proof assumed that in the Strutinsky approach the plateau condition could be fulfilled.

In the WK expansion, the diagonal part of the the Bloch density [21,22] is

$$C(\boldsymbol{r},\beta)=\frac{1}{4\pi^{3/2}\beta^{3/2}}\left(\frac{2M}{\hbar^2}\right)^{3/2}e^{-\beta V(\boldsymbol{r})}\left\{1-\frac{\hbar^2\beta^2}{12M}\left[\nabla^2V(\boldsymbol{r})-\frac{\beta}{2}(\nabla V(\boldsymbol{r}))^2\right]+\ldots\right\}. \tag{9}$$

The spatial density is obtained by using the inverse Laplace transform

$$\rho(\boldsymbol{r},\varepsilon)=\mathcal{L}^{-1}_{\beta\to\varepsilon}\left(\frac{C(\boldsymbol{r},\beta)}{\beta}\right), \tag{10}$$

and the particle number integral is given by

$$N(\varepsilon)=\int\rho(\boldsymbol{r},\varepsilon)\;d^3r. \tag{11}$$

Keeping only the two leading terms in the curly bracket in Eq. (9), the WK particle number equation can be expressed explicitly in terms of the single-particle potential

$$N_{sc}(\varepsilon)=\frac{4}{3\pi}\left(\frac{2M}{\hbar^2}\right)^{\frac{3}{2}}\int^{r_{\rm sc}(\varepsilon)}r^2\left\{(\varepsilon-V)^{\frac{3}{2}}-\frac{\hbar^2}{32M}\frac{\nabla^2V}{(\varepsilon-V)^{\frac{1}{2}}}\right\}dr. \tag{12}$$

The integral in Eq. (12) is cut off at the classical turning point, $r_{\rm sc}(\varepsilon)$, defined by the relation $V(r_{\rm sc})=\varepsilon$. (For the inclusion of the spin-orbit term see Ref. [20].) The semi-classical value of the Fermi energy, $\lambda_{\rm sc}$, can be determined from the particle number equation $N_{\rm sc}(\lambda_{\rm sc})=N$.

The semi-classical level density is defined as

$$g_{\rm sc}(\varepsilon)=\frac{dN_{\rm sc}(\varepsilon)}{d\varepsilon}. \tag{13}$$

Here, it is worth reminding that the semi-classical level density is defined only for $\varepsilon>V_0$, where V_0 denotes the bottom of the potential well. That is, $g_{\rm sc}(\varepsilon)$=0 if $\varepsilon<V_0$. An explicit expression for $g_{\rm sc}(\varepsilon)$ in terms of a WK expansion can be found in, e.g., Ref. [23].

It is to be noted that Eqs. (9-13) are valid for any smooth potential regardless whether it is infinite *or not*. Often, the semi-classical level density is defined in terms of the partition function $Z(\beta) = \int C(\boldsymbol{r},\beta)\ d^3r$. However, there is a difficulty: $Z(\beta)$ diverges for finite potentials [23]. In practical calculations it is possible to overcome this serious problem by an appropriate modification of the potential at large disstances. Formally, this procedure is equivalent to placing an infinite potential well (a box with soft walls) at very large distances from the classical region [23].

Since the particle-number integral (12) depends only on the potential in the classical region, where $V_0<\varepsilon<V_{\rm B}$, the quantity $N_{\rm sc}(\varepsilon)$ is well defined for energies which are not too close to the top of the potential well $V_{\rm B}$ where the semi-classical expansion breaks down (see Appendix A). Hence the total number of particles can be calculated without the explicit use of the partition function; there is no need at all to put the system into a box in the case of a finite potential.

The total energy of the system of non-interacting particles is

$$E = \int_{-\infty}^{\lambda} \varepsilon g(\varepsilon) d\varepsilon = \lambda N - \int_{-\infty}^{\lambda} N(\varepsilon) d\varepsilon. \tag{14}$$

By means of Eqs. (11) and (10), E can be written as

$$E = \lambda N - \int \mathcal{L}^{-1}_{\beta\to\lambda}\left(\frac{C(\boldsymbol{r},\beta)}{\beta^2}\right) d^3r. \tag{15}$$

Here it is assumed that the order of the integration with respect to ε (and $\boldsymbol{r}$) and the inverse Laplace transform can be interchanged. Using Eq. (15), the semi-classical smoothed binding energy can be written as

$$\tilde{E}_{\rm sc} = \lambda_{\rm sc} N - \int \mathcal{L}^{-1}_{\beta\to\lambda_{\rm sc}}\left(\frac{C_{\rm sc}(\boldsymbol{r},\beta)}{\beta^2}\right) d^3r, \tag{16}$$

where the notation $C_{\rm sc}(\boldsymbol{r},\beta)$ means that only the terms which are not a higher order than $\hbar$ are kept in the WK expansion of $C(\boldsymbol{r},\beta)$. As it was discussed in [20], for the determination of $\lambda_{\rm sc}$ it is enough to keep the terms of order $\hbar^{-1}$ in Eq.(9). The explicit expression for the smoothed energy is quite lengthy and can be found in Ref. [20].

IV. GENERALIZED SHELL-CORRECTION METHOD

The impact of the particle continuum on shell corrections has been investigated numerically in Ref. [12] for neutrons in ^{208}Pb and ^{298}114 by explicit calculation of the continuum part of the level density, Eq. (4). They have shown that, by taking into account contributions from the neutron continuum up to ∼100 MeV in ^{208}Pb, the plateau condition (8) could be met (see Ref. [2] for an updated discussion of the continuum contribution in ^{208}Pb). Based on this early exercise, it was generally *assumed* that the plateau condition could be fulfilled for finite potentials provided that the continuum part was included. A systematic study of this assumption is given in Sec. V B.

The lack of systematic studies using the continuum level density is due to the fact that these calculation are quite cumbersome. Except for some special cases, the solution of the

radial differential equation can be done only numerically. The calculation of the phase shifts and the continuum level density along the real energy axis should be carried out with great care. In general, the use of an extremely fine energy step is required in order to collect contributions from narrow resonances. Recently, this difficulty has been overcome by applying a new method which uses Gamow states [2]. A Gamow resonance is a generalized eigenstate of the radial Schrödinger equation corresponding to a complex energy eigenvalue $w_i = \varepsilon_i - i\Gamma_i$ (for bound states Γ_i=0). The wave function of a Gamow resonance is regular at r=0 and has purely outgoing asymptotics with a discrete complex wave number.

In the new method (see Ref. [2] for details), the smoothed level density $\tilde{g}(\varepsilon)$ can be written with the help of the Cauchy theorem as a sum over bound and resonant states, and an integral along a contour L in the complex energy plane:

$$\tilde{g}(\varepsilon) = \sum_i f\left(\frac{\varepsilon - w_i}{\gamma}\right) + \int_L dw\ g_{\rm c}(w) f\left(\frac{\varepsilon - w}{\gamma}\right). \tag{17}$$

In Eq. (17), the summation runs over all the bound states and those resonances which are above the contour L and below the real energy axis.

Thanks to the Cauchy theorem, the level density as given by Eq. (17) has only real part (the imaginary parts of the two terms in the r.h.s. of Eq. (17) should cancel out exactly). Furtermore, $\tilde{g}(\varepsilon)$ should be independent of the shape of the contour L. However, since the calculations are carried out numerically, the exact cancellation of the imaginary parts is always slightly violated and, in addition, the sum of the real parts slightly depends on the shape of the contour. For example, if the contour L is extended to the area of the complex energy plane with large imaginary energies (Im(w)<–5 MeV) then broad resonances, i.e., those with large Γ_i-values should be included. As a result, both terms in the r.h.s. of Eq. (17) would acquire large imaginary parts which would not cancel completely due to the numerical errors. Therefore, the best strategy is to choose the contour in such a way that it would include only narrow resonances. With this choice the final result is practically independent of the shape of the contour, and the imaginary part of $\tilde{g}(\varepsilon)$ is negligible (it is the order of 10^{-4} or less). Three examples of contours L are shown in Fig. 1.

With a reasonable choice for the contour L, the Gamow resonances give the major contribution from the continuum; the contour integral gives the remaining (small) part. From the smoothed level density (17) one can determine $\tilde{\lambda}$ and $\tilde{E}_{\rm s.p.}$ using Eqs. (7) and (6), respectively.

It is worth noting that another, commonly used method of calculating the continuum level density is based on the discretization procedure. Here, one assumes that the nucleus is placed inside a very large box (cf. the discussion in Sec. III on the application of the semi-classical expansion to finite potentials). Since the properties of the nucleus itself must not depend on the box size, one has to re-normalize the level density by subtracting the contribution from the free-gas states [13,24–27]. In Refs. [13,27], the discretization method was applied to investigate the accuracy of the semi-classical expression (13) for several commonly used potentials, and a good agreement was found in all cases.

V. RESULTS

A. Details of calculations

In the actual calculations, we have used the average Woods-Saxon (WS) potential, which contains a central part, a spin-orbit term, and a Coulomb potential for protons. The Coulomb potential has been assumed to be that of a charge $(Z-1)e$ distributed with the diffused charge density. We employed the set of WS parameters introduced in Ref. [28], and the charge density form factor was taken in the WS form. (See Ref. [4] for details pertaining to the single-particle model.)

The poles of the S-matrix, i.e. the eigenvalues w_i, have been calculated by solving the radial equation numerically using the computer code GAMOW [29]. The contour L has been chosen to lie far from these poles. This ensures that the energy dependence of phase shifts along the path is smooth; hence one can use relatively large energy steps. The phase shifts of scattering states along the path L have been calculated by solving the radial equation numerically using the unpublished code ZSCAT in which the complex Coulomb routine COULCC was used [30].

As an illustrative example, the distribution of eigenvalues w_i for the stable nucleus ^{90}Zr (neutrons), neutron drip-line nucleus ^{122}Zr (neutrons), and proton-rich nucleus ^{180}Pb (protons) is shown in Fig. 1, together with the contours L used for calculating the level density (17). In the case of ^{90}Zr, there are four poles close to the $\varepsilon = 0$ threshold. They are: $p_{1/2}$ (w=0.2$-i$0.19 MeV), $f_{5/2}$ (w=2.1$-i$0.34 MeV), $i_{13/2}$ (w=3.7$-i$0.004 MeV), and $h_{9/2}$ (w=3.9$-i$0.03 MeV). As seen in Fig. 1, only the Gamow states with the smallest widths, i.e., $i_{13/2}$ and $h_{9/2}$, have been considered explicitly in the level density calculations; a contribution from the remaining eigenstates has been accounted for by the integral along the path L, i.e., by the second term in Eq. (17). For the neutron-rich nucleus ^{122}Zr, the number of near-threshold Gamow states increases. Here, three Gamow resonances: $f_{7/2}$ (w=0.7$-i$0.02 MeV), $h_{9/2}$ (w=3.2$-i$0.03 MeV), and $i_{13/2}$ (w=4.5$-i$0.02 MeV) have been used to define the contour that includes them in Fig. 1b. As seen in Fig. 1(c), the distribution of the proton Gamow eigenvalues in ^{180}Pb is different. Due to the presence of the Coulomb barrier, there appear many very narrow resonances even at relatively high energies, i.e. above 10 MeV; therefore we have chosen in this case a contour that includes these narrow resonances.

The energy dependence of neutron phase shifts in ^{122}Zr and proton phase shifts in ^{180}Pb along the contour L is illustrated in Fig. 2. Here are shown the real and imaginary parts of

$$N_{\rm c}(w) = \frac{1}{\pi}\sum_{l,j}(2j+1)\delta_{lj}(w). \tag{18}$$

According to Eq. (4), $N_{\rm c}$ can be interpreted as the "continuum particle number" along the contour. As expected, the energy dependence of $N_{\rm c}$ along the path is very smooth. It is also seen that the imaginary part of $N_{\rm c}$ is small since the contour does not go far from the real energy axis.

The WK calculations in this paper follow those of Ref. [4] except for the treatment of the proton average field. Since the combined WS and Coulomb potentials give rise to a non-monotonic field, in this study we had to employ a modified treatment of some of the terms in the WK expansion according to Ref. [31].

B. Modified plateau condition

In order to check the dependence of the smoothed single-particle energy on γ and p, we made systematic calculations of the shell energy by varying these parameters within reasonable ranges. Figure 3 shows three typical examples of our analysis of neutron shell corrections. The plateau condition is satisfied fairly well for the super-heavy nucleus $^{298}114_{184}$. (This nucleus was previously studied in Ref. [12].) Here, for each p value, δE possesses a local minimum in γ, and the minimum energy changes little with p. However, in the cases of ^{146}Gd and ^{90}Zr, it is impossible to assign a definite value to the neutron shell correction. The situation for ^{146}Gd and ^{90}Zr shown in Fig. 3 should be considered as typical; the plateau condition (8) is seldom satisfied. Therefore, we conclude that the *proper treatment of the continuum level density does not guarantee that the plateau condition is fulfilled.*

In the cases where the plateau condition was approximately satisfied, like in Fig. 3(a), we found a strong correlation between the values of γ and p . In particular, the behavior of $\tilde{g}(\varepsilon)$ as a function of ε was found to be very similar for different values of p and γ corresponding to local minima in δE. Moreover, the dependence of $\tilde{g}(\varepsilon)$ was found to be almost linear in a wide range of ε below $\tilde{\lambda}$. We also checked that for the cases when the plateau condition could not be satisfied [see, e.g., Figs. 3(b,c)], the approximate linearity of $\tilde{g}(\varepsilon)$ was valid. It is worthwhile to point out that for the harmonic oscillator potential, the average level density behaves as ε^2, while for the finite square well potential, the leading terms behave as $\sqrt{\varepsilon}$ [16,13]. Hence, a local linear behavior of $\tilde{g}(\varepsilon)$ for a finite WS potential is not unexpected. This observation suggests that an alternative recipe for defining shell correction for finite potentials, not based on the plateau condition but rather on the behavior of the smooth level density, may be possible.

It is well known that the realistic value of the smoothing parameter has to lie in a certain energy interval [23]. The value of γ should be large enough to wipe out shell effects in the energy range of a typical distance between shells:

$$\gamma > \hbar\Omega. \tag{19}$$

On the other hand, its upper limit is defined by the number of states considered in the calculations, i.e.,

$$\gamma \ll \varepsilon_{\max} - \tilde{\lambda}, \tag{20}$$

and by the energy distance between the Fermi level and the bottom of the well [15], i.e.,

$$\gamma \ll \tilde{\lambda} - V_0. \tag{21}$$

In practice, the optimal value of γ for a given p is found by the following procedure. First we choose the energy interval $[\varepsilon_l, \varepsilon_u]$ which is lying below $\tilde{\lambda}$ and is wider than the average shell distance, e.g., ε_u–ε_l>1.5 $\hbar\Omega$. In this energy interval, we perform the least squares fit to the smoothed level density assuming a linear dependence of $\tilde{g}(\varepsilon)$ on ε. The search for optimal γ begins at a small γ value below $\hbar\Omega$ where the shell fluctuations are still present, and then γ is gradually increased until the first minimum in δE is found at γ_p. This γ_p corresponds to the smallest value of γ for a given p that smooths out the shell fluctuations. The corresponding shell correction, $\delta E = \delta E_p$, is taken as the optimal shell correction for

this p. This procedure is repeated for higher values of p. If variations of δE_p with p are small, then the mean value of δE_p represents the shell correction obtained in this modified Strutinsky method. The uncertainty of the procedure is given by the r.m.s. error $\sigma \equiv \sigma(\delta E)$.

The smoothed level densities $\tilde{g}(\varepsilon)$, calculated using the above procedure, are displayed in Fig. 4 for three different values of p=6, 10, and 14. Since $\tilde{g}(\varepsilon)$ is practically independent of the value of p we amplified the differences by presenting in Fig. 4 the ratios of the level densities to $\tilde{g}(\varepsilon)$ belonging to $p = 10$.

The shell energy is also practically independent of the value of p. Table I displays the calculated proton and neutron shell-correction energies and the corresponding r.m.s. errors. Since σ increases when going to lighter nuclei where the condition (21) does not hold, we limited calculations to nuclei heavier than ^{40}Ca. The calculations were performed for nuclei close to the stability valley and for nuclei with extreme N/Z ratios (both neutron-rich and proton-rich). It is seen that the r.m.s. error in δE is always less than 250 keV (also for the cases such as ^{90}Zr or ^{146}Gd where the plateau condition could not be met). Another source of theoretical uncertainty lies in the choice of the fitting range $[\varepsilon_l, \varepsilon_u]$. In particular, the selection of ε_u plays a role for weakly bound nuclei with very small values of $\tilde{\lambda}$. In practice, in order to guarantee that the fitting region does not overlap with the threshold area, we have adopted the value of $\varepsilon_u = \tilde{\lambda} - \hbar\Omega$ and $\varepsilon_l = \varepsilon_u - 1.5\hbar\Omega$. In order to estimate the associated theoretical error, we have performed a set of calculations for well-bound nuclei assuming a larger value of ε_u, namely $\varepsilon_u = \tilde{\lambda}$. The average deviation in δE between the two sets of calculations is around 400 keV. We believe that this number represents a fair estimate of the uncertainty of our method.

C. Comparison with the semiclassical method

As a next step, we performed the detailed comparison of the generalized Strutinsky method with the WK expansion. Table I displays the shell correction $\delta E_{\rm sc} = E_{\rm s.p.} - \tilde{E}_{\rm sc}$ calculated using the WK method, together with the difference $\Delta \equiv \delta E - \delta E_{\rm sc}$. In most cases $\Delta > 0$. That is, the semi-classical method yields the average single-particle energy $\tilde{E}_{\rm sc}$ which is greater than $\tilde{E}_{\rm s.p.}$ obtained in the generalized Strutinsky method. The average value of Δ is about 0.45 MeV and the maximal deviation is about 1.8 MeV for neutrons and 0.9 MeV for protons. These deviations exhibit large fluctuations with particle number, and they are significantly larger than the uncertainty of the generalized Strutinsky smoothing procedure. Considering the excellent agreement between the shell energies calculated in the Strutinsky and the WK methods obtained previously [20], and the existing proof of the equivalence between these two methods [17], the large magnitudes of Δ in Table I seem to be surprising.

In order to understand this discrepancy, we analyze the behavior of smoothed single-particle level densities obtained in both methods. The semi-classical level density has been obtained by means of Eq. (13), i.e., by calculating the derivative of $N_{\rm sc}(\varepsilon)$.

Smoothed level densities $\tilde{g}(\varepsilon)$ and $g_{\rm sc}(\varepsilon)$ are compared in Figs. 4 and 5 for ^{146}Gd (neutrons) and ^{208}Pb (protons), respectively. The behavior of average single-particle densities displayed in Fig. 5 shows a generic pattern characteristic of a WS-like potential well [13,27]. Namely, $\tilde{g}(\varepsilon)$ increases monotonically with ε reaching the maximum value around the ε=0 threshold for the neutrons (and around V_B, i.e. the top of the Coulomb barrier for the protons), and then it smoothly falls down reflecting the increasing contribution from the

free-gas states. As discussed in Sec. V B, there exists a wide energy region in which $g_{\rm sc}(\varepsilon)$ increases fairly linearly with ε. In general, $\tilde{g}(\varepsilon)$ and $g_{\rm sc}(\varepsilon)$ are very close except for the bottom of the potential well ($\varepsilon \approx V_0$) and close to the top of the potential barrier.

Considering the low-energy region, there are problems with both methods. The Strutinsky smoothed density is non-zero for $\varepsilon < V_0$, i.e., in the classically forbidden region. Here, the inequality (21) cannot be met and the averaging method breaks down [15]. Also, there are serious questions regarding the applicability of the semi-classical treatment close to the $\varepsilon = V_0$ limit. The $\hbar^{-1}$ term in the WK expansion of the semi-classical level density [related to the second term in the integral (12)] gives rise to the singularity around the bottom of the well. (For a square well potential this singularity behaves as $(\varepsilon - V_0)^{-1/2}$.) As discussed in Ref. [23], in the strict treatment of $g_{\rm sc}(\varepsilon)$, there appears a correction to the level density, proportional to the Dirac delta $\delta(\varepsilon - V_0)$. This additional term, usually ignored in calculations, partly corrects for a pathological behavior around the bottom of the well by introducing a small shift in the Fermi level $\lambda_{\rm sc}$ [16]. Table I displays the Fermi energies $\tilde{\lambda}$ and $\lambda_{\rm sc}$. Usually, the Fermi levels are very close; for well-bound nuclei the difference is less than 100 keV. Although small, this shift partly contributes to the calculated values of Δ (e.g., for protons in ^{208}Pb).

Another major deviation between $\tilde{g}(\varepsilon)$ and $g_{\rm sc}(\varepsilon)$ is seen in the energy region close to the $\varepsilon = 0$ threshold in the neutrons, and around the top of the proton Coulomb barrier. Here, the reason for this abnormal behavior is our semi-classical approximation. As discussed in Appendix A, the WK neutron level density $g_{\rm sc}(\varepsilon)$ diverges as $\ln(-\varepsilon)/\sqrt{-\varepsilon}$ when $\varepsilon \to 0$. For protons, the singularity is even more severe: $g_{\rm sc}(\varepsilon)$ diverges as $(V_{\rm B} - \varepsilon)^{-1}$ around the top of the barrier.

The pathological behavior of $g_{\rm sc}(\varepsilon)$ around zero energy is the reason for the largest deviations Δ seen in Table I for the neutron case (e.g., $\Delta = 1.39$ MeV for ^{78}Ni, and it is greater than 1 MeV for the Zr isotopes with $A = 110, 122, 124$). These nuclei are weakly bound (as shown by their low Fermi energies), and the level density around the Fermi level, $g_{\rm sc}(\tilde{\lambda})$, is affected by the threshold effect.

In order to understand the systematic behavior of Δ in Table I, neutron shell corrections and Fermi energies for the Zr isotopes are shown in Fig. 6 as functions of N. The calculations were performed using the single-particle potential corresponding to ^{90}Zr. The associated smoothed level densities are shown in Fig. 7. It is seen that although the general pattern of δE is similar in the generalized shell-correction method and WK approach, Δ exhibits the oscillatory behavior as a function of particle number. The agreement between δE and $\delta E_{\rm sc}$ is very good up to $N \sim 70$ ($\tilde{\lambda} \sim -4$ MeV), but it is spoiled at large neutron numbers where Δ systematically increases. Indeed, above point "C" in Fig. 7, the semi-classical level density diverges, and it does not yield a good estimate of the shell correction.

For the protons, the "dangerous" threshold region of $g_{\rm sc}$ is shifted to higher energies due to the presence of the Coulomb barrier (see Fig. 5). That explains why the differences between the Strutinsky and WK results are smaller for the protons than for the neutrons. For instance, for the proton drip-line nucleus ^{100}Sn the agreement between two methods is surprisingly good in spite of the fact that $\tilde{\lambda} = 0.72$ MeV. Since in actual nuclei (both particle-bound and in proton emitters) the proton Fermi level is significantly lower than $V_{\rm B}$, the divergent behavior of proton $g_{\rm sc}$ around the top of the Coulomb barrier has no practical importance.

VI. CONCLUSIONS

This paper introduces a new method of calculating the nuclear shell energy. The generalized Strutinsky procedure fully takes into account the effect of the particle continuum. Although the traditional plateau condition can seldom be met for finite potentials, the proposed method makes it possible to define shell correction unambiguously. A conservative estimate of the uncertainty in δE obtained using the new smoothing procedure is $\sim$400 keV. This error can be considered as small.

In most cases, the results of the generalized Strutinsky procedure are in good agreement with those of the semi-classical WK method. Significant deviations have been obtained for neutron-rich nuclei for which the neutron Fermi energy is low (λ>–4 MeV). This discrepancy has been tracked back to the singularity in the WK level density around the top of the potential barrier. The density $\tilde{g}(\varepsilon)$ obtained in the generalized Strutinsky method nicely interpolates through the threshold region (see also Refs. [13,27]). Other advantages of the new method are: (i) its applicability to potentials with discontinuous derivatives (e.g., the Coulomb potential of a uniform charge distribution and a folded-Yukawa potential) where the standard WK expansion cannot be carried out, and (ii) simple generalization to the deformed case where the semiclassical expansion becomes awkward [4].

Finally, let us comment on the difference Δ between shell corrections obtained in both methods. There are several factors which contribute to Δ. In addition to the threshold anomaly mentioned above, other factors are: (i) the shift between the Fermi levels caused by the different behavior of the level densities at the bottom of the potential well, (ii) the assumption of the local linearity of the smoothed level density, and (iii) the systematic errors accumulated during numerical calculations. For protons, our calculations give $|\Delta|$<900 keV in all cases considered. Here, the main source of the difference is the deviation between the level densities around the bottom of the potential well, i.e., factor (i). For neutrons with $\tilde{\lambda}$<–4 MeV, the value of $|\Delta|$ is even smaller: $|\Delta|$<600 keV. The largest deviations approaching 2 MeV have been obtained for the neutron drip-line nuclei such as ^{122}Zr. Considering the analysis presented in this study, it has to be concluded that the excellent agreement found in Ref. [20] ($|\Delta|\sim$100 keV) is fortuitous. According to our results in Table I, for nuclei discussed by these authors, i.e., ^{208}Pb and ^{208}114, the difference Δ is indeed very small. However, in other cases deviations are larger.

ACKNOWLEDGMENTS

This research was supported in part by the Hungarian National Research Fund (OTKA T17298), the Swedish Royal Academy of Sciences, the U.S. Department of Energy under Contract Nos. DE-FG02-96ER40963 (University of Tennessee), DE-FG05-87ER40361 (Joint Institute for Heavy Ion Research), DE-AC05-96OR22464 with Lockheed Martin Energy Research Corp. (Oak Ridge National Laboratory), the Institute of Atomic Physics, Bucharest, and by the Polish Committee for Scientific Research.

APPENDIX A: NEAR-THRESHOLD BEHAVIOR OF THE SEMICLASSICAL LEVEL DENSITY

In the WK method, the semiclassical level density $g_{\rm sc}(\varepsilon)$ can be written as

$$g_{\rm sc}(\varepsilon) = g_{\rm TF}(\varepsilon) + g_{-1}(\varepsilon), \tag{A1}$$

where $g_{\rm TF}(\varepsilon)$ is the Thomas-Fermi (TF) level density and $g_{-1}(\varepsilon)$ is the WK correction term (of the order of $\hbar^{-1}$). By employing Eqs. (13) and (12), one can write $g_{\rm sc}(\varepsilon)$ as a derivative of the particle number with respect to ε:

$$g_{\rm TF}(\varepsilon) = \frac{dN_{\rm TF}}{d\varepsilon}, \quad g_{-1}(\varepsilon) = \frac{dN_{-1}}{d\varepsilon}. \tag{A2}$$

In Eq. (A2), $N_{\rm TF}$ is the TF particle number,

$$N_{\rm TF}(\varepsilon) = \frac{4}{3\pi}\left(\frac{2M}{\hbar^2}\right)^{\frac{3}{2}} \int^{r_{\rm sc}(\varepsilon)} (\varepsilon - V)^{\frac{3}{2}} r^2 dr, \tag{A3}$$

while the $\hbar^{-1}$ WK term is

$$N_{-1}(\varepsilon) = -\frac{1}{12\pi}\left(\frac{2M}{\hbar^2}\right)^{\frac{1}{2}} \int^{r_{\rm sc}(\varepsilon)} \frac{\nabla^2 V}{\sqrt{\varepsilon - V}} r^2 dr. \tag{A4}$$

As usual, the classical turning point is defined by the relation $V(r_{\rm sc}(\varepsilon)) = \varepsilon$.

The pathological behavior of $g_{\rm sc}(\varepsilon)$ close to the top of the potential barrier can be attributed to the singularity in the $g_{-1}(\varepsilon)$ term. To examine this divergence, let us consider the integral

$$I(\varepsilon) \equiv \int_{\tilde{r}}^{r_{\rm sc}(\varepsilon)} \frac{\nabla^2 V}{\sqrt{\varepsilon - V}} r^2 dr, \tag{A5}$$

where it has been assumed that $V(r)$ is an increasing function of r on an interval $[\tilde{r}, r_{\rm sc}]$, and $\tilde{r}$ is a fixed radius ($\tilde{r} < r_{\rm sc}$).

By substituting $x = V(r)$, $I(\varepsilon)$ can be written as:

$$I(\varepsilon) = \int_{\tilde{x}}^{\varepsilon} \frac{\eta(x)}{\sqrt{\varepsilon - x}} dx, \tag{A6}$$

where $\tilde{x} = V(\tilde{r})$ and

$$\eta(x) \equiv r^2 \frac{\nabla^2 V}{V'}|_x = \left(r^2 \frac{V''}{V'} + 2r\right)|_x. \tag{A7}$$

The singularity at $x = \varepsilon$ in the integrand in Eq. (A6) can be eliminated by performing a partial integration:

$$I(\varepsilon) = 2\eta(\tilde{x})\sqrt{\varepsilon - \tilde{x}} + 2\int_{\tilde{x}}^{\varepsilon} \eta'(x)\sqrt{\varepsilon - x} dx. \tag{A8}$$

The first term in Eq. (A8) does not cause any problems around the particle threshold and can be neglected in the following. Hence the behavior of $g_{-1}(\varepsilon)$ around the top of the barrier is governed by the integral

$$I'(\varepsilon) \approx \int_{\tilde{x}}^{\varepsilon} \frac{\eta'(x)}{\sqrt{\varepsilon - x}} dx. \tag{A9}$$

1. Woods Saxon potential: neutron case

For neutrons in a WS potential, the particle threshold appears at ε=0. In the vicinity of the threshold, the potential energy can be approximated by

$$V(r) \approx \tilde{x} \exp\left(-\frac{r-\tilde{r}}{a}\right), \tag{A10}$$

and the classical radius is

$$r(x) = \tilde{r} + a \ln\left(\frac{\tilde{x}}{x}\right). \tag{A11}$$

In the limit $\varepsilon \to 0$, the function $\eta(x)$ in Eq. (A7) can be written as:

$$\eta(x) = 2r(x) - r^2(x)/a \approx -r^2(x)/a. \tag{A12}$$

Hence

$$\eta'(x) \approx 2\frac{r(x)}{x} \tag{A13}$$

and

$$I'(\varepsilon) \approx 2\int_{\tilde{x}}^{\varepsilon} \frac{\ln\left(\frac{\tilde{x}}{x}\right)}{x\sqrt{\varepsilon - x}} dx. \tag{A14}$$

The above integral can be easily calculated. Around ε=0, it behaves as

$$\ln\left(\frac{\varepsilon}{\tilde{x}}\right) / \sqrt{\frac{\varepsilon}{\tilde{x}}}, \tag{A15}$$

and this is the asymptotic behavior of $g_{\rm sc}(\varepsilon)$ around the neutron threshold.

The behavior of $g_{\rm sc}(\varepsilon)$ for the neutrons in ^{120}Sn at $\varepsilon\sim$0 is displayed in Fig. 8(a). It is seen that the semiclassical density diverges according to the law given by Eq. (A15).

2. Finite potential barrier: proton case

For potentials with finite barriers, such as the sum of WS and Coulomb potentials, the particle threshold appears at the top of the barrier, ε=$V_{\rm B}$. Around the barrier top, the potential energy can be expanded as

$$V(r) \approx V_{\rm B} - \alpha\frac{1}{2}(r - r_{\rm B})^2, \tag{A16}$$

where $\alpha = -V''(r_{\rm B})$.

For $\varepsilon \approx V_{\rm B}$, the function $\eta(x)$ in Eq. (A7) can be written as:

$$\eta(x) \approx -\frac{r^2(x)}{r_{\rm B} - r(x)}. \tag{A17}$$

Consequently,

$$\eta'(x) \approx -\frac{r^2(x)}{\alpha[r_{\rm B} - r(x)]^3}, \tag{A18}$$

and the leading term in $I'(\varepsilon)$ takes the form

$$I'(\varepsilon) \to \int_{\tilde{x}}^{\varepsilon} \frac{1}{(V_{\rm B} - x)^{3/2}\sqrt{\varepsilon - x}} dx. \tag{A19}$$

The above integral can be easily evaluated. Around ε=$V_{\rm B}$ it behaves as

$$\frac{1}{V_{\rm B} - \varepsilon}, \tag{A20}$$

and this gives the asymptotic behavior of $g_{\rm sc}(\varepsilon)$ around the top of the Coulomb barrier.

The behavior of $g_{\rm sc}(\varepsilon)$ for the protons in ^{120}Sn around ε=$V_{\rm B}$ is displayed in Fig. 8(b). It is seen that around the top of the barrier the semi-classical density diverges according to the law given by Eq. (A20). Of course, the WK contribution (A4) to the particle number also diverges when $\varepsilon \to V_{\rm B}$. This result is by no means surprising; the semi-classical approximation breaks down if the gradient of the potential at the turning point vanishes, and this happens precisely around the top of the barrier.

REFERENCES

[1] J. Dobaczewski and W. Nazarewicz, Phil. Transactions, in press, 1997; nucl-th/9707049.
[2] N. Sandulescu, O. Civitarese, R.J. Liotta, and T. Vertse, Phys. Rev. **C55**, 1250 (1997).
[3] T. Vertse, R.J. Liotta, and E. Maglione, Nucl. Phys. **A584**, 13 (1995).
[4] W. Nazarewicz, T. R. Werner, and J. Dobaczewski, Phys. Rev. **C50**, 2860 (1994).
[5] V.M. Strutinsky, Nucl. Phys. **A95**, 420 (1967).
[6] V.M. Strutinsky, Nucl. Phys. **A122**, 1 (1968).
[7] M. Bolsterli, E.O. Fiset, J.R. Nix, and J.L. Norton, Phys. Rev. **C5**, 1050 (1972).
[8] P. Möller and J.R. Nix, Nucl. Phys. **A361** (1981) 117.
[9] G.E. Uhlenbeck and E. Beth, Physica **3**, 729 (1936).
[10] E. Beth and G.E. Uhlenbeck, Physica **4**, 915 (1937)
[11] Wing-fai Lin, Phys. Rev. **C2** (1970) 871.
[12] C.K. Ross and R.K. Bhaduri, Nucl. Phys. **A188**, 566 (1972).
[13] S. Shlomo, Nucl. Phys. **A539**, 17 (1992).
[14] A. Bohr and B.R. Mottelson, Nuclear Structure, vol. 1 (W.A. Benjamin, New York, 1969).
[15] M. Brack and H.C. Pauli, Nucl. Phys. **A207**, 401 (1973).
[16] R.K. Bhaduri and C.K. Ross, Phys. Rev. Lett. **27**, 606 (1971).
[17] B.K. Jennings, Nucl. Phys. **A207**, 538 (1973).
[18] B.K. Jennings, R.K. Bhaduri, and M. Brack, Phys. Rev. Lett. **A34**, 228 (1975).
[19] B.K. Jennings and R.K. Bhaduri, Nucl. Phys. **A237**, 149 (1975).
[20] B.K. Jennings, R.K. Bhaduri, and M. Brack, Nucl. Phys. **A253**, 29 (1975).
[21] M. Brack and R.K. Bhaduri, *Semiclassical Physics* (Addison-Wesley, Reading, Mass., 1997).
[22] R.K. Bhaduri, Phys. Rev. Lett. **39**, 329 (1977).
[23] B.K. Jennings, Ann. Phys. **84**, 1 (1974).
[24] D.L. Tubbes and S.E. Koonin, Astrophys. J. **232**, L59 (1979).
[25] A.K. Kerman and S. Levit, Phys. Rev. **C24**, 1029 (1981).
[26] D.R. Dean and U. Mosel, Z. Phys. **A322**, 647 (1985).
[27] S. Shlomo, V.M. Kolomietz, and H. Dejbakhsh Phys. Rev. **C55**, 1972 (1997).
[28] J. Dudek, Z. Szymański, and T.R. Werner, Phys. Rev. **C23**, 920 (1981).
[29] T. Vertse, K.F. Pál, and Z. Balogh, Comput. Phys. Commun. **27**, 309 (1982).
[30] I.J. Thompson and A.R. Barnett, Comput. Phys. Commun. **36**, 363 (1985).
[31] A.K. Dutta and J.M. Pearson, Pramāṇa **29**, 379 (1987).

TABLES

TABLE I. Shell correction δE , the r.m.s. error σ, and the Fermi level $\tilde{\lambda}$ calculated using the generalized Strutinsky method with continuum. The corresponding semi-classical quantities: shell correction $\delta E_{\rm sc}$ and Fermi level $\lambda_{\rm sc}$ are also shown together with the difference $\Delta \equiv \delta E - \delta E_{\rm sc}$. All energies are in MeV.

			Neutrons			
Nucleus	δE	σ	$\tilde{\lambda}$	$\delta E_{\rm sc}$	$\lambda_{\rm sc}$	Δ
^{78}Ni	-2.83	0.183	-2.64	-4.22	-2.51	1.39
^{90}Zr	-7.19	0.100	-9.63	-6.82	-9.77	-0.37
^{96}Zr	0.24	0.016	-7.32	0.82	-7.37	-0.58
^{104}Zr	6.57	0.056	-4.79	6.48	-4.71	0.09
^{106}Zr	5.97	0.039	-4.23	5.56	-4.13	0.41
^{108}Zr	5.76	0.150	-3.69	4.94	-3.57	0.82
^{110}Zr	4.49	0.029	-3.17	3.45	-3.05	1.04
^{122}Zr	-4.61	0.056	-0.32	-6.40	-0.44	1.79
^{124}Zr	-2.91	0.052	0.12	-4.39	-0.12	1.47
^{132}Sn	-8.70	0.023	-4.50	-8.94	-4.42	0.24
^{146}Gd	-10.09	0.118	-9.77	-9.85	-9.89	-0.24
^{208}Pb	-11.37	0.063	-5.50	-11.23	-5.56	-0.13
^{298}114	-8.44	0.090	-4.83	-8.63	-4.81	0.19
			Protons			
Nucleus	δE	σ	$\tilde{\lambda}$	$\delta E_{\rm sc}$	$\lambda_{\rm sc}$	Δ
^{48}Ni	-2.11	0.084	-0.16	-1.94	-0.08	-0.17
^{90}Zr	1.96	0.222	-6.65	1.45	-6.84	0.51
^{100}Sn	-7.31	0.083	0.72	-7.01	0.61	-0.30
^{132}Sn	-6.02	0.081	-13.24	-6.65	-13.31	0.63
^{146}Gd	5.27	0.247	-3.98	4.51	-4.12	0.77
^{180}Pb	-7.72	0.016	-0.81	-8.57	-0.87	0.85
^{208}Pb	-6.73	0.028	-7.16	-7.33	-7.22	0.60

FIGURES

FIG. 1. The distribution of Gamow energy eigenvalues, w_i in the (Re(w), Im(w)) plane for (a) the stable nucleus ^{90}Zr (neutron eigenvalues), (b) neutron drip-line nucleus ^{122}Zr (neutron eigenvalues), and (c) proton-rich nucleus ^{180}Pb (proton eigenvalues). The contours L used in Eq. (17) to calculate the smoothed level density in the generalized shell-correction method are also shown. Only the Gamow states with w_i lying above the contour are included in the leading term in Eq. (17).

FIG. 2. The energy dependence of the "continuum particle number" (18) for the neutrons in ^{122}Zr (a) and the protons in ^{180}Pb (b) along the contours L of Fig. 1(b,c). The energy dependence of $N_{\rm c}$ along the path is very gradual. The fluctuations in $N_{\rm c}$ can be attributed to the presence of near-lying Gamow states.

FIG. 3. Shell correction for the neutrons in (a) ^{298}114, (b) ^{146}Gd, and (c) ^{90}Zr obtained using the generalized Strutinsky averaging procedure as a function of the smoothing range parameter γ for various orders of the curvature correction: p=8 (dotted line), p=12 (dot-dashed line), and p=16 (solid line). The continuum contribution to the level density has been calculated using the method described in Ref. [2]. The gray line shows the result of the semi-classical Wigner-Kirkwood approach.

FIG. 4. Comparison of the smoothed level densities calculated using the generalized Strutinsky method (SM) and the Wigner-Kirkwood method (WK) for (a) the neutrons in ^{146}Gd and (b) the protons in ^{208}Pb. The densities are normalized to the Strutinsky density $\tilde{g}(\varepsilon)$ calculated with the curvature correction p=10. Semi-classical level densities and Strutinsky level densities calculated with p=6 and 14 are shown by dotted, dot-dashed, and dashed lines, respectively. It is seen that the result of the Strutinsky smoothing is practically p-independent. The Fermi levels $\tilde{\lambda}$ (SM) and $\lambda_{\rm sc}$ (WK) are indicated, together with the value of the potential depth V_0.

FIG. 5. Comparison of the smoothed level densities calculated using the generalized Strutinsky method (solid line, p=10 variant) and the Wigner-Kirkwood method (dotted line) for the neutrons in ^{146}Gd (top) and the protons in ^{208}Pb (bottom).

FIG. 6. Neutron shell corrections and Fermi energies as a function of N calculated in the SM and WK models using the single-particle potential of ^{90}Zr. The corresponding smoothed level densities are shown in Fig. 7.

FIG. 7. Same as in Fig. 5 except for the neutrons in ^{90}Zr. The points at which the difference between SM and WK level densities, δg, changes sign are marked by "A", "B", and "C". The oscillatory behavior of δg is responsible for the oscillatory behavior of Δ as a function of particle number, as shown in Fig. 6.

FIG. 8. The divergent behavior of $g_{\rm sc}(\varepsilon)$ for the neutrons (a) and the protons (b) in ^{120}Sn around the particle threshold. It is seen that the semi-classical approximation breaks down in the vicinity of the threshold. The densities scaled according to Eqs. (A15): $1000 g_{\rm sc}(\varepsilon)/[\ln(\tilde{\varepsilon})/\sqrt{\tilde{\varepsilon}}]$ (where $\tilde{\varepsilon} = \varepsilon/V_0$), and Eq. (A20): $1000 g_{\rm sc}(\varepsilon)/[1/\tilde{\varepsilon}]$ (where $\tilde{\varepsilon} = (\varepsilon - V_{\rm B})/V_0$) are shown in the insets.

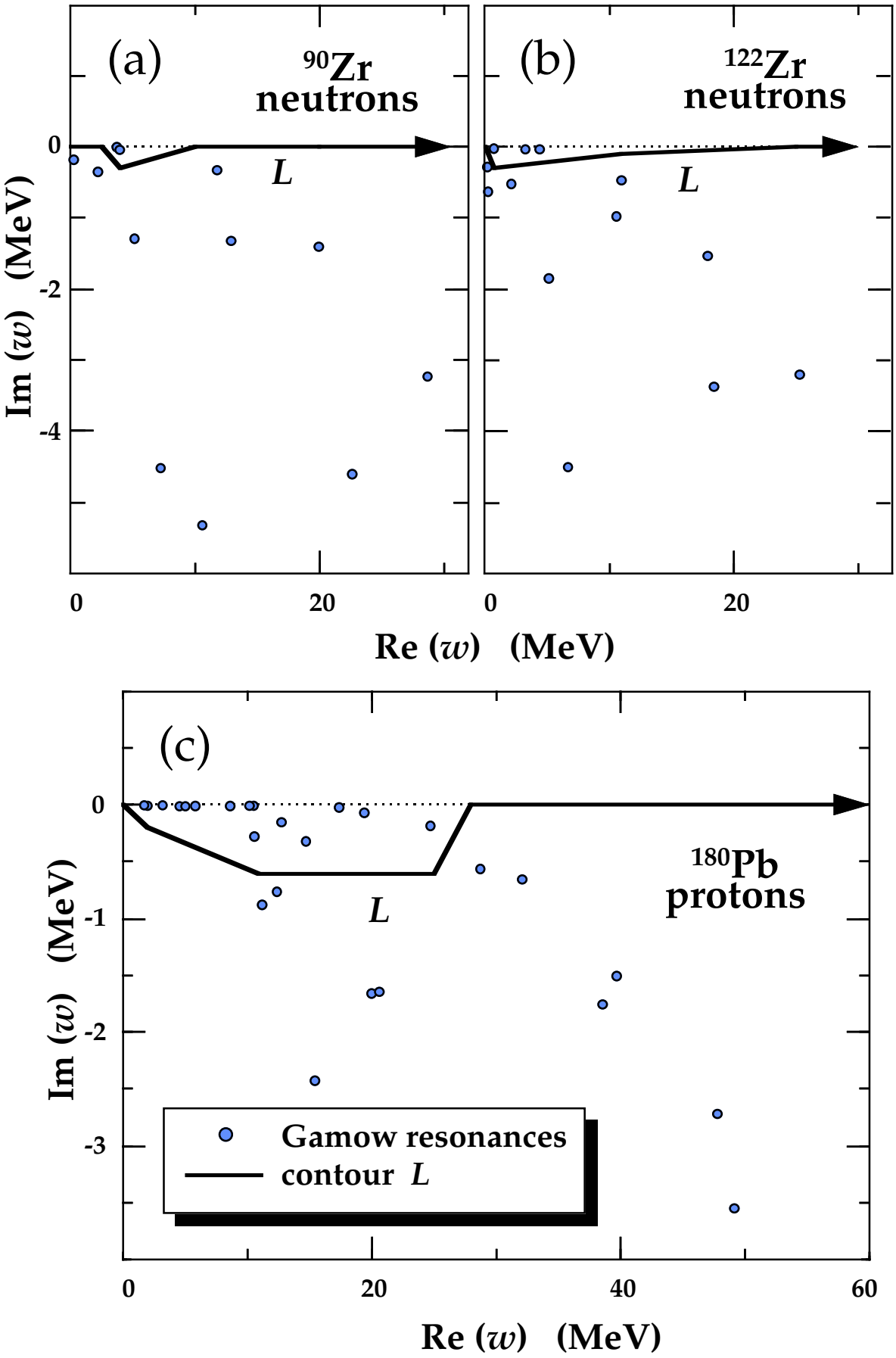
(a)
^{90}Zr
neutrons
(b)
^{122}Zr
neutrons
L
L
0
-2
-4
Im (w) (MeV)
0
20
0
20
Re (w) (MeV)
(c)
0
-1
-2
-3
Im (w) (MeV)
L
^{180}Pb
protons
Gamow resonances
contour L
0
20
40
60
Re (w) (MeV)

Fig. 1

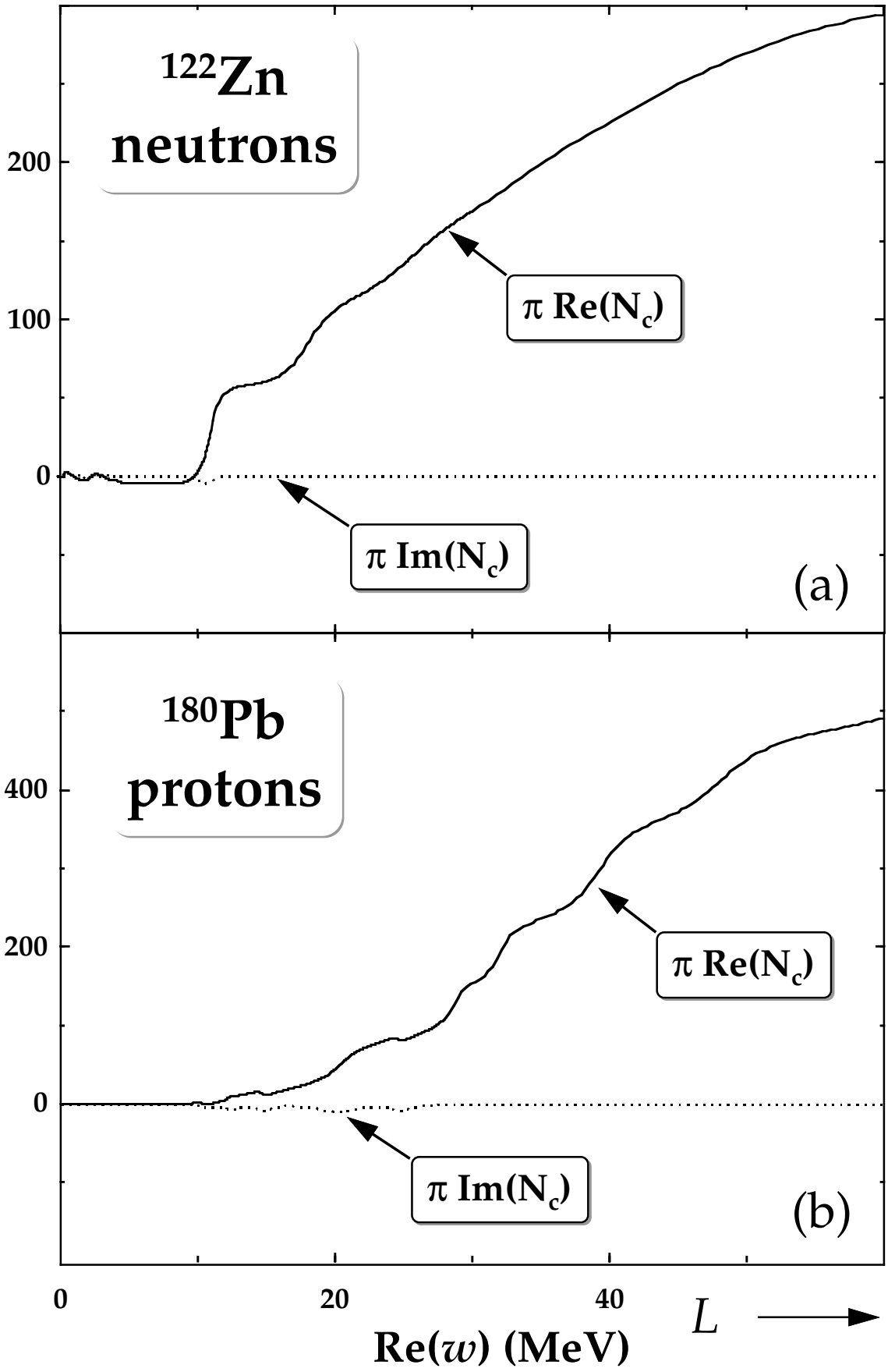
^{122}Zn
neutrons
200
100
0
π Re(N$_c$)
π Im(N$_c$)
(a)
^{180}Pb
protons
400
200
0
π Re(N$_c$)
π Im(N$_c$)
(b)
0
20
40
Re(w) (MeV)
L

Fig. 2

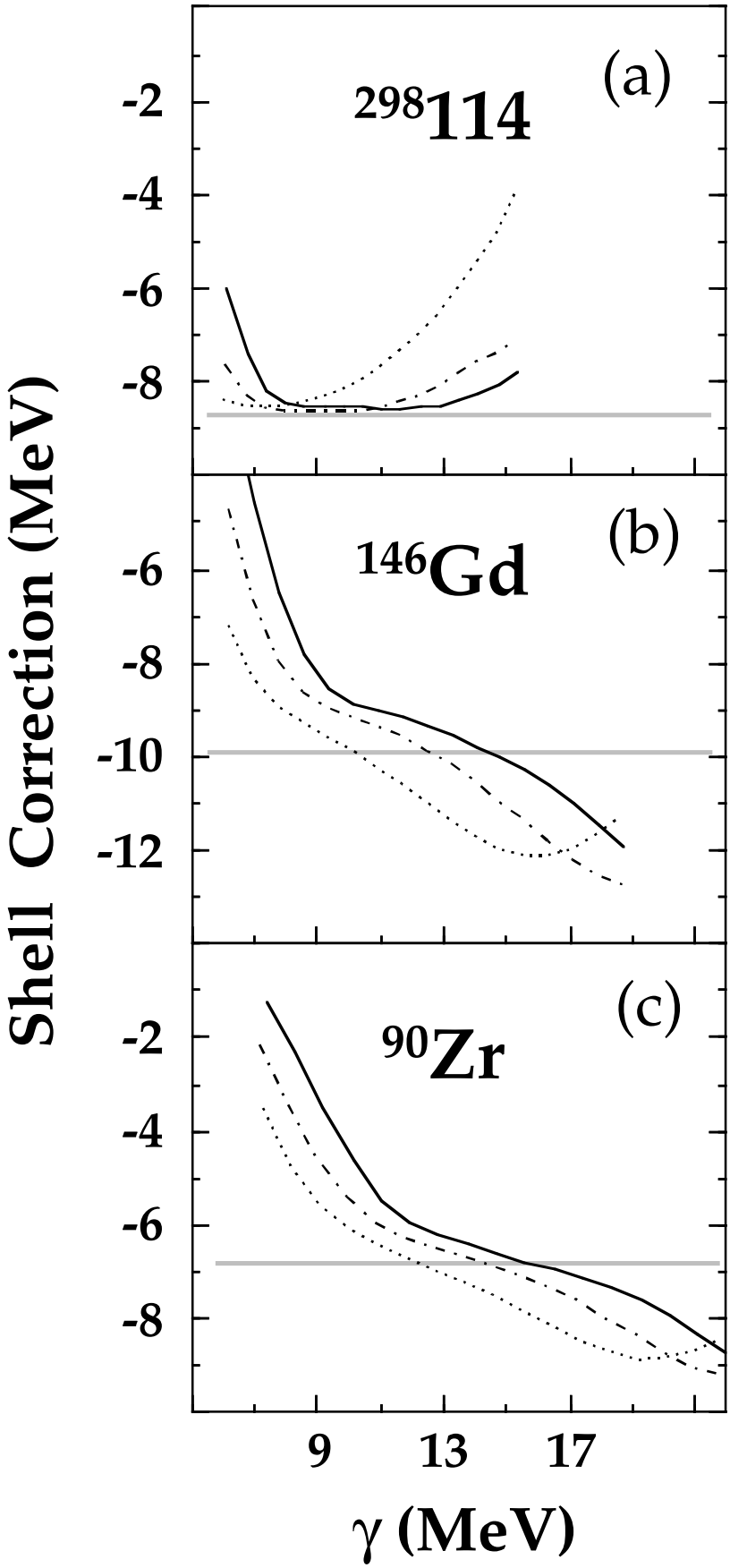
(a)
^{298}114
-2
-4
-6
-8
(b)
^{146}Gd
-6
-8
-10
-12
(c)
^{90}Zr
-2
-4
-6
-8
9
13
17
Shell Correction (MeV)
γ (MeV)

Fig. 3

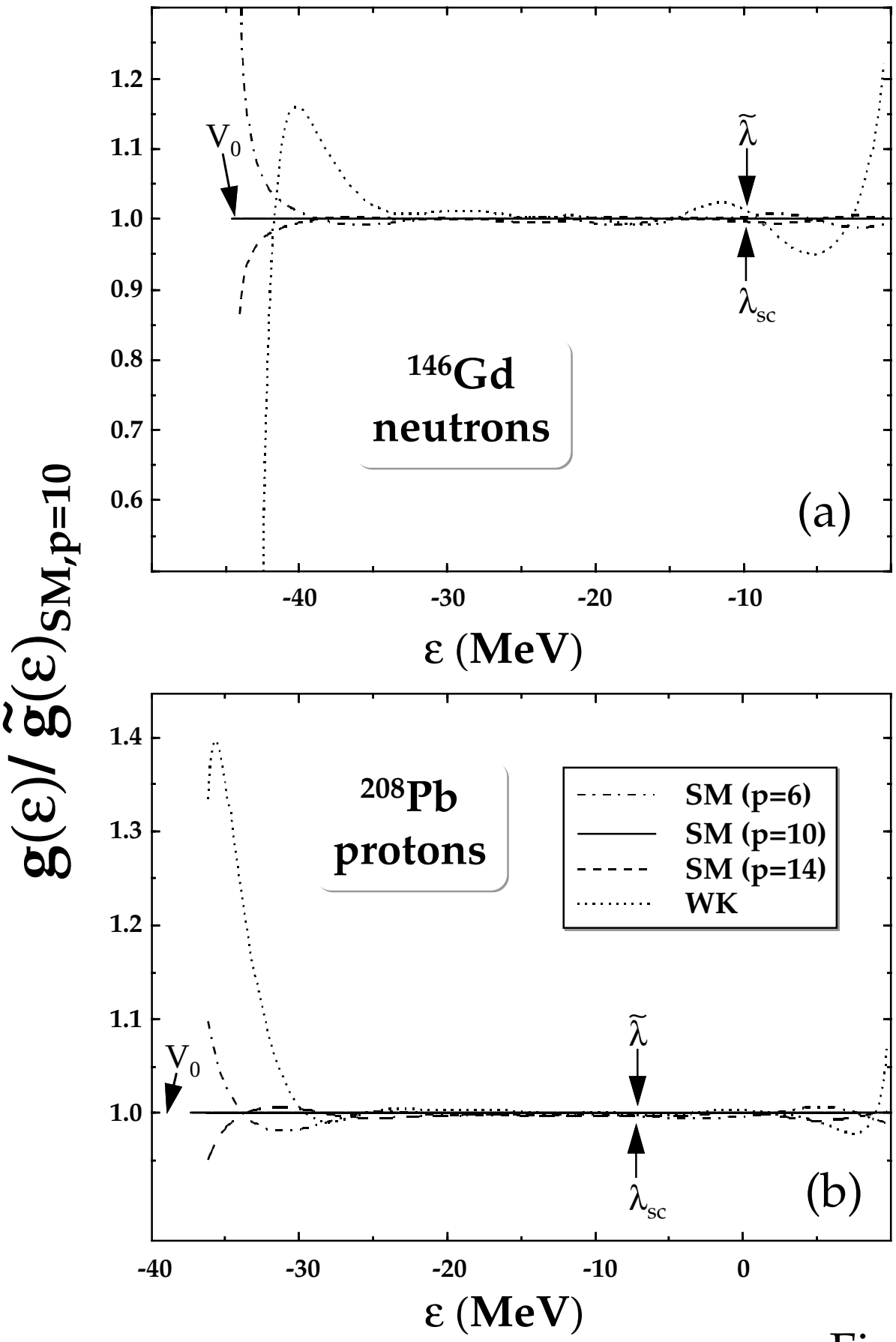
g(ε)/ g̃(ε)SM,p=10
1.2
1.1
1.0
0.9
0.8
0.7
0.6
V0
λ̃
λsc
146Gd
neutrons
(a)
-40
-30
-20
-10
ε (MeV)
1.4
1.3
1.2
1.1
1.0
208Pb
protons
SM (p=6)
SM (p=10)
SM (p=14)
WK
V0
λ̃
λsc
(b)
-40
-30
-20
-10
0
ε (MeV)

Fig. 4

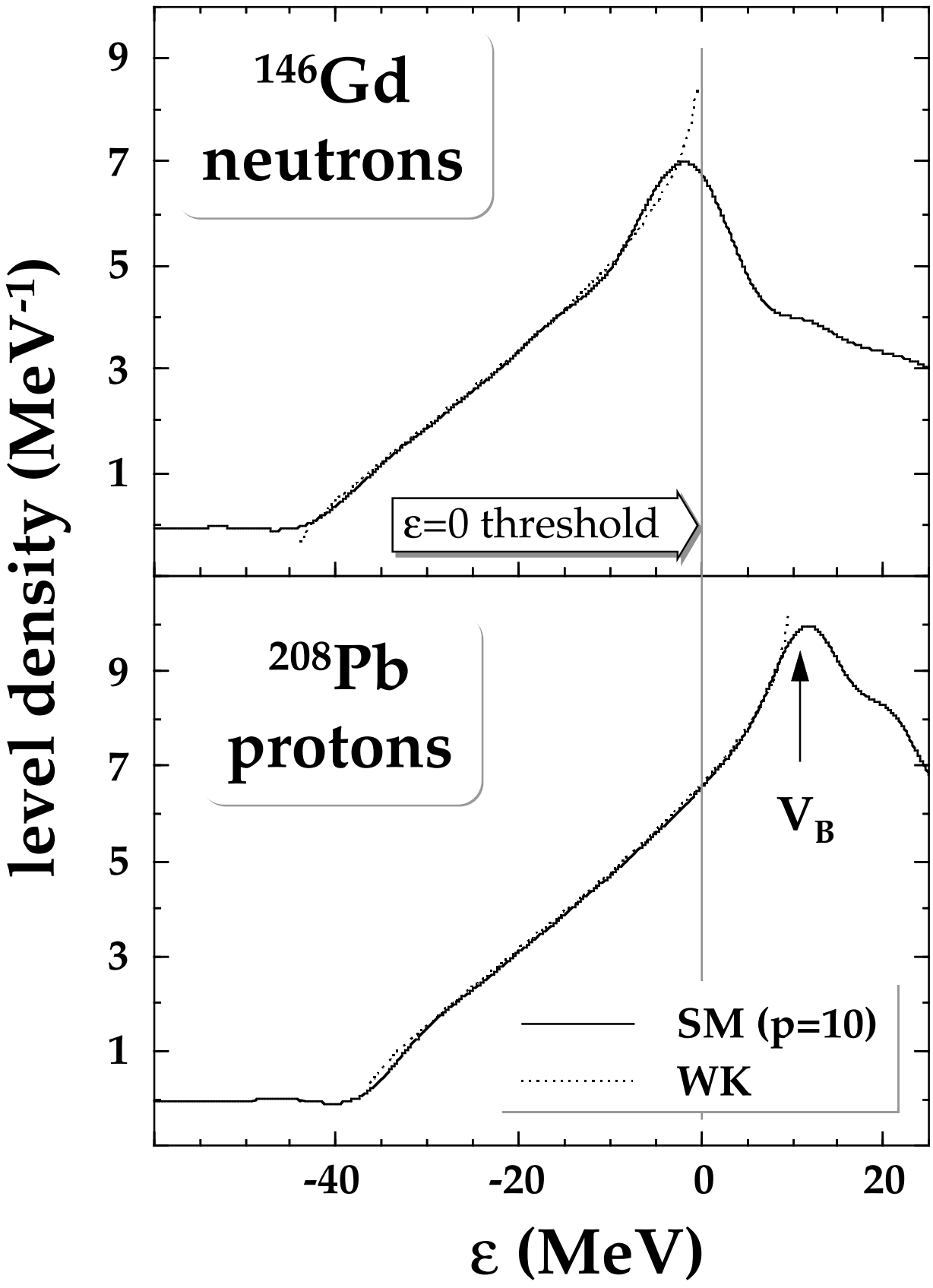
level density (MeV-1)
9
7
5
3
1
146Gd
neutrons
ε=0 threshold
208Pb
protons
V_B
SM (p=10)
WK
-40
-20
0
20
ε (MeV)

Fig. 5

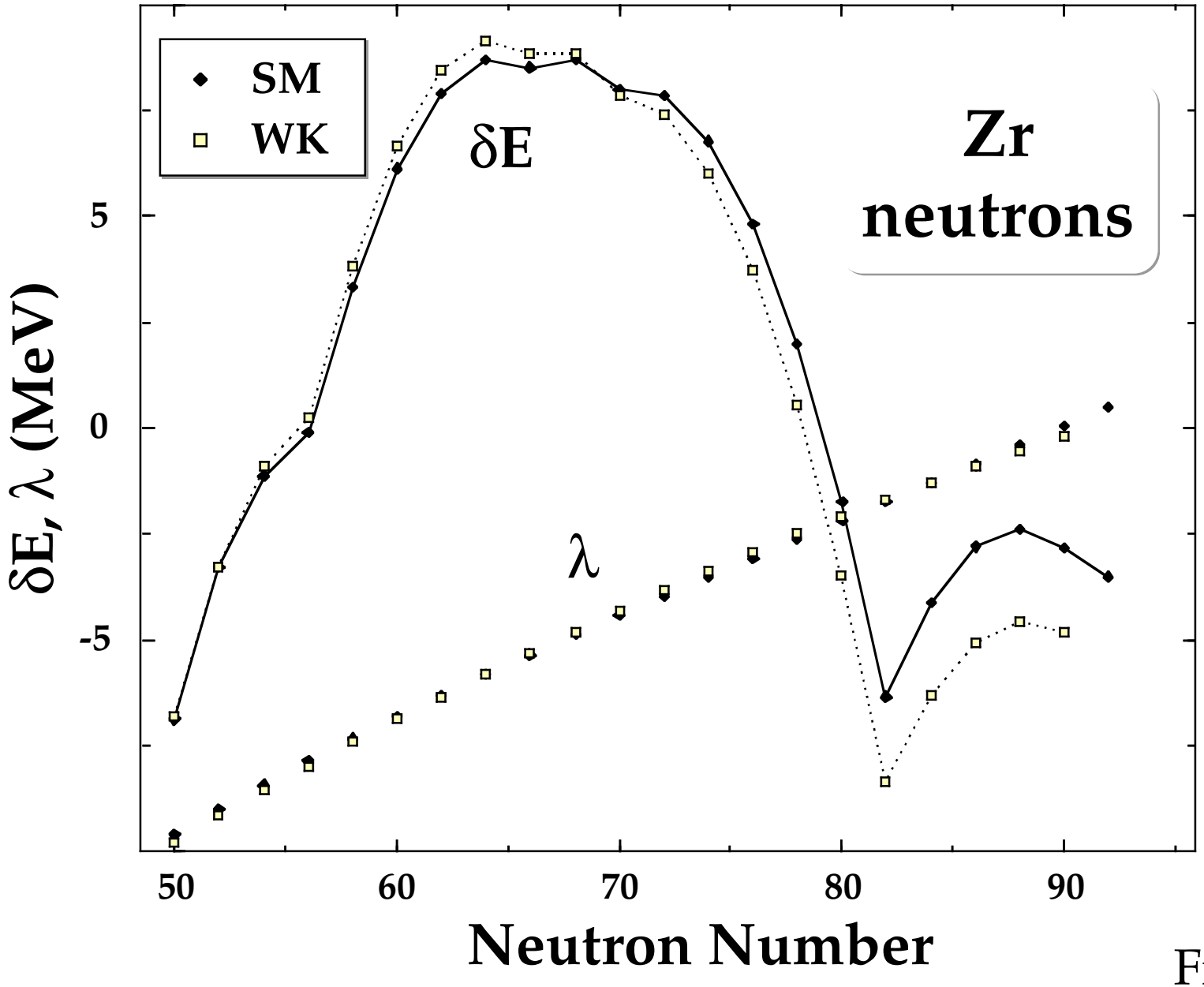

Fig. 6

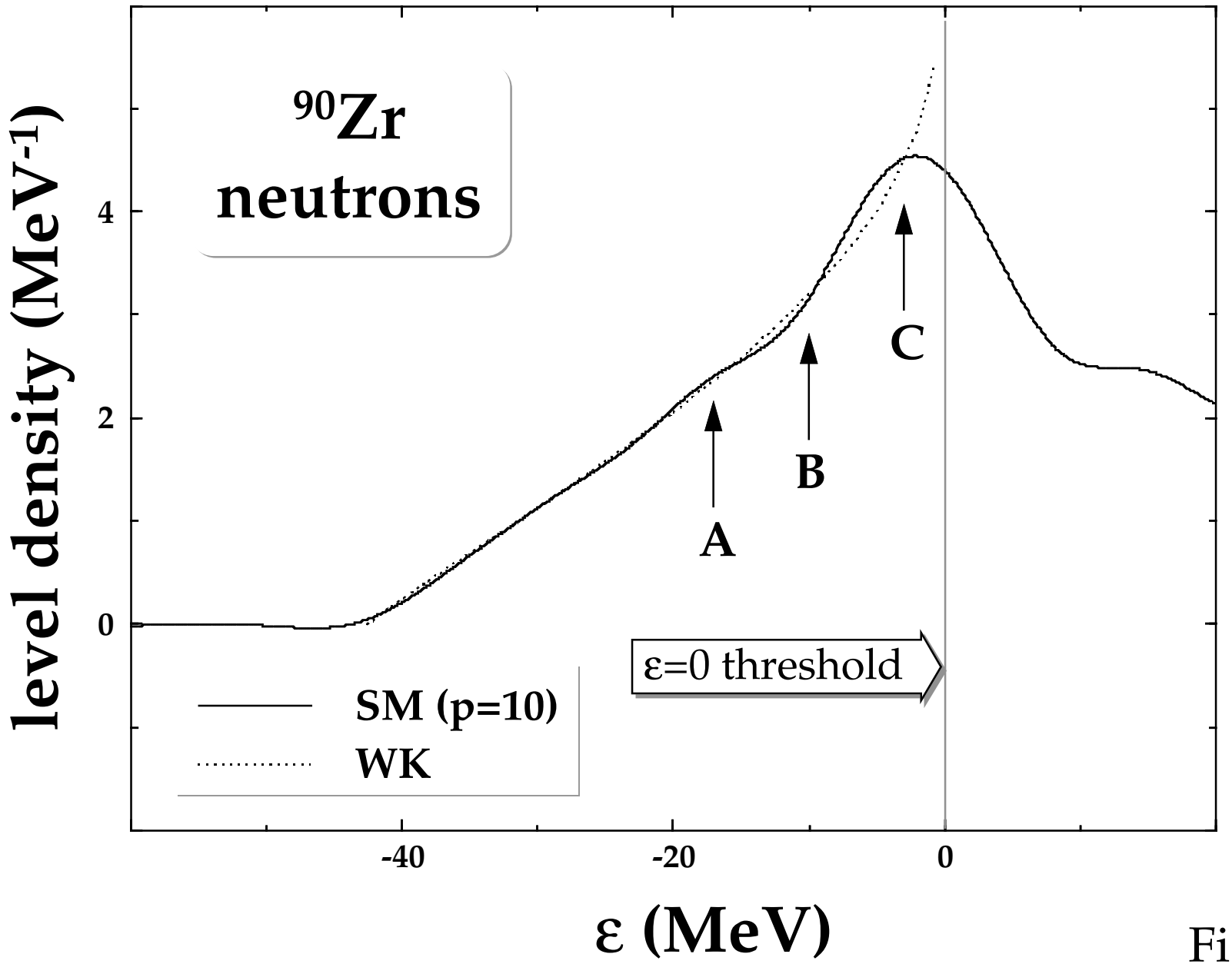
^{90}Zr
neutrons
level density (MeV^{-1})
4
2
0
A
B
C
ε=0 threshold
SM (p=10)
WK
-40
-20
0
ε (MeV)

Fig. 7

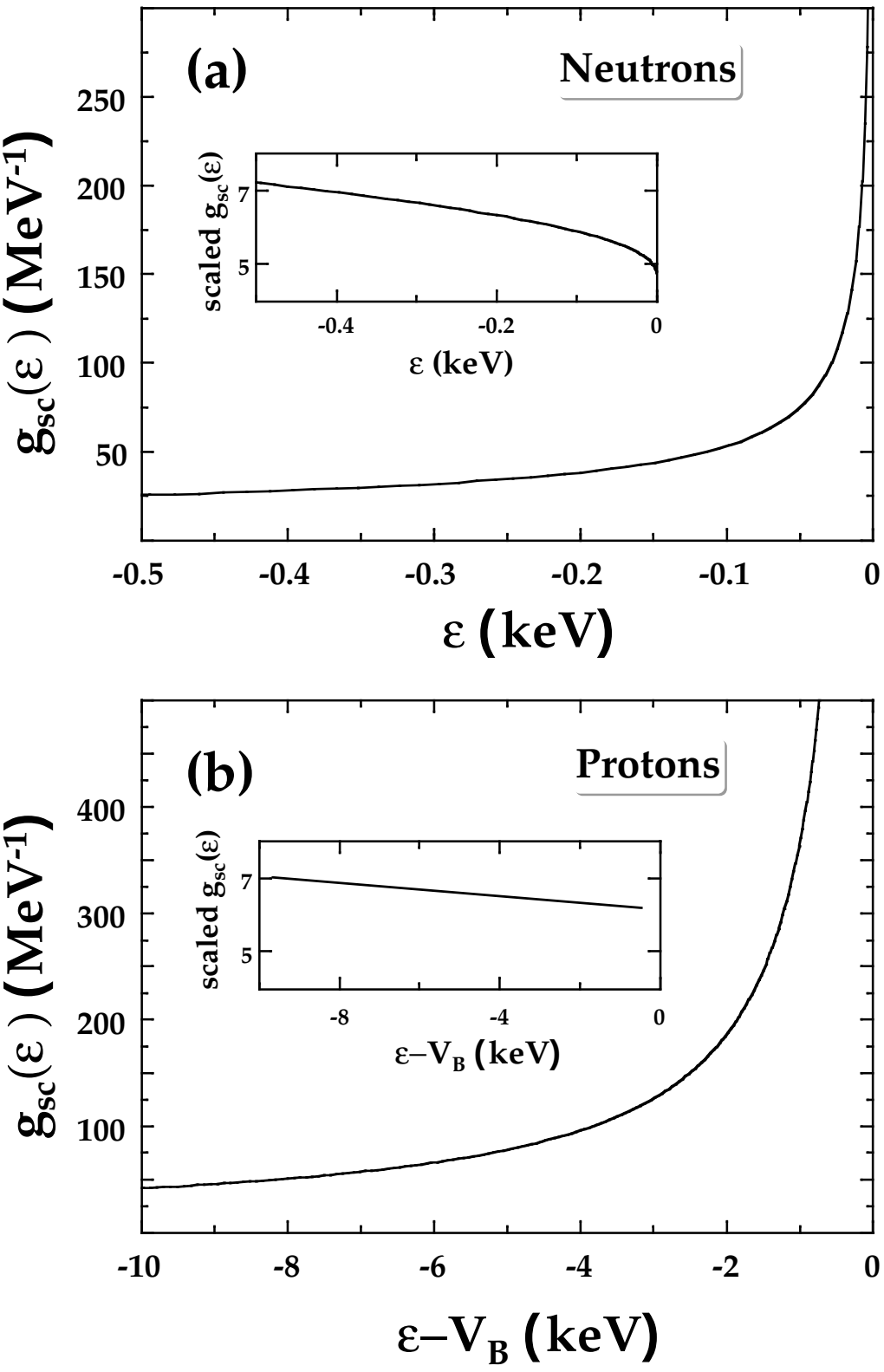
(a)
Neutrons
250
200
150
100
50
$g_{sc}(\varepsilon)$ (MeV^{-1})
-0.5
-0.4
-0.3
-0.2
-0.1
0
ε (keV)
scaled $g_{sc}(\varepsilon)$
7
5
-0.4
-0.2
0
ε (keV)
(b)
Protons
400
300
200
100
$g_{sc}(\varepsilon)$ (MeV^{-1})
-10
-8
-6
-4
-2
0
ε–V_B (keV)
scaled $g_{sc}(\varepsilon)$
7
5
-8
-4
0
ε–V_B (keV)

Fig. 8